

A Generic Regression Framework for Pose Recognition on Color and Depth Images

Wenye He

Cascaded regression method is a fast and accurate method on finding 2D pose of objects in RGB images. It is able to find the accurate pose of objects in an image by a great number of corrections on the good initial guess of the pose of objects. This paper explains the algorithm and shows the result of two experiments carried by the researchers. The presented new method to quickly and accurately predict 3D positions of body joints from a single depth image, using no temporal information. We take an object recognition approach, designing an intermediate body parts representation that maps the difficult pose estimation problem into a simpler per-pixel classification problem. Our large and highly varied training dataset allows the classifier to estimate body parts invariant to pose, body shape, clothing. Finally, we generate confidence-scored 3D proposals of several body parts by re-projecting the classification result and finding local modes.

Introduction

Detection and localization provide a helpful function in computer vision. Detection finds out whether an object is contained in the image, while localization tells people which specific place of the image an object is in. For example, there is an image of tree. Detection can tell us whether a bird is in the image and localization shows where the bird it is. Localization could answer whether the bird flies in the sky or stays on the tree. More specifically, localization enable us to know which

groups of pixels represent a bird in the image.

On the other hand, robust interactive human body tracking has different applications that include gaming, human computer interaction, security, telepresence and even the health care. The task has recent been simplified by the introduction of real time depth cameras. However even the best existing system has limitations. Until the launch of Kinect, none ran at interactive rates on consumer hardware while handling a full range of human body shapes and sizes undergoing general body motions. Detecting body parts from a single depth image is a challenging task from a small set of 3D position candidates for each skeletal joint³. They focused on pre-frame initialization and recovery is designed to complement any appropriate tackling algorithm

In this paper, we demonstrate an algorithm to answer a question Is an object o with pose θ located in the image I . In their work, after making a raw guess of the pose of an object in a set of image, they use cascaded pose regression to detect which image has such the object and locate which region in the image contains the object. Pose-indexed features² and its assumed weak invariance are used in the algorithm. Furthermore, random ferns⁴ regressors are applied in CPR. The system runs at 200 frames per second on consumer hardware. The evaluation shows high accuracy on both synthetic and real test sets, and investigates the effect of several training parameters. They achieved state of the art accuracy in our comparison with related work and demonstrate improved generalization over exact whole-skeleton nearest neighbour matching.

Related Works

This paper uses features to achieve pose estimate. In computer vision, features have great functions. The popular use of features is recognition. Paul and Michael⁵ use rectangle features for object detection. Lowe⁶ present an approach to identify objects using highly distinctive and scale - invariant features, and has been applied for many applications¹². Features also help people in 3D model retrieval. Ryutarou et al.⁷ obtain 3D model using salient local visual features. In this paper, researchers apply pose-indexed features² whose concept is proposed by Francois and Donald to estimate pose. Early work in pose estimation contains active contour models⁹, 2D range scans matching¹⁰, and active appearance models¹¹. In recent work, pose estimation is employed to reconstruct 3D shape¹⁴ and detect and localize object¹⁶. [13] use the marginal statistics of unlabelled data to improve pose estimation. [18, 8] proposed a local mixture of Gaussian Processes to regress human pose. Auto-context was used in [17] to obtain a coarse body part labelling. [19] track a hand clothed in a colored glove. Our system could be automatically inferring the colors of a virtual colored suit from a depth image and used for many RGB-D applications, such as virtual reality¹⁵.

Method

This section describes how Cascaded Pose Regression works. First of all, the researchers create an image model $G : \mathcal{O} \times \Theta \rightarrow \mathcal{I}$. The model show how an image $I \in \mathcal{I}$ is constructed from an object $o \in \mathcal{O}$ and pose $\theta \in \Theta$. Given that poase estimate is suppose to be unique in the model, $\mathcal{G}(o_1, \theta_1) = \mathcal{G}(o_2, \theta_2)$ iff $o_1 = o_2$ and $\theta_1 = \theta_2$. Moreover, the operator \circ is designed for

combination of two poses. The researchers write a formula for a new pose composed of θ_1 and θ_2 , $\theta = \theta_1 \circ \theta_2$. $\bar{\theta}$ is set as the inverse of θ , and e as the identity element. A function to calculate relative error between two poses is formed, $d : \Theta \times \Theta \rightarrow \mathcal{R}$ where $d(\theta_1, \theta_2)$ depends on $\bar{\theta}_1 \circ \theta_2$ or equivalently that $d(\theta_\delta \circ \theta_1, \theta_\delta \circ \theta_2) = d(\theta_1, \theta_2)$ for all $\theta_1, \theta_2, \theta_\delta \in \Theta$.

Pose-indexed features and weak invariance are introduced in CPR. A pose-indexed features is a function, $h : \Theta \times \mathcal{I} \rightarrow \mathcal{R}$. h is weakly invariant if

$$h(\theta, G(o, e)) = h(\theta_\delta \circ \theta, G(o, \theta_\delta)),$$

where $\forall \theta, \theta_\delta \in \Theta$, or equivalently,

$$h(\theta_1, G(o, \theta_2)) = h(\theta_\delta \circ \theta_1, G(o, \theta_\delta \circ \theta_2)),$$

where $\forall \theta_1, \theta_2, \theta_\delta \in \Theta$. Each pose-indexed feature is composed of control point features and pose. Each control feature, h_{p_1, p_2} , is computed as the difference of two pixels, p_1 and p_2 at predefined image locations, so $h_{p_1, p_2}(I) = I(p_1) - I(p_2)$ where $I(p)$ is the grayscale value of image I at location p . Therefore, taking pose θ into account, the researchers define an pose-indexed feature $h_{p_1, p_2}(\theta, I) = I(H_\theta p_1) - I(H_\theta p_2)$, where H_θ is an associated 3×3 homography matrix. Figure 1 shows pose-indexed features in mice and zebra fish.

After introducing pose-indexed features and weakly invariance, the evaluation and training algorithm on CPR is demonstrated here and is shown in Figures 2 and Figure 3. The full formula to evaluate CPR is $\theta^t = \theta^{t-1} \circ R^t(h^t(\theta^{t-1}, I))$, where $t = 1 \dots T$ and R is a cascaded regressor trained in Figure 3, given an input pose, initial pose, θ^0 and an image I , outputting θ^T . The full evaluating procedures is shown by testing images in Figure 4.

The objective for training a new regressor is to reduce the difference between the true pose and

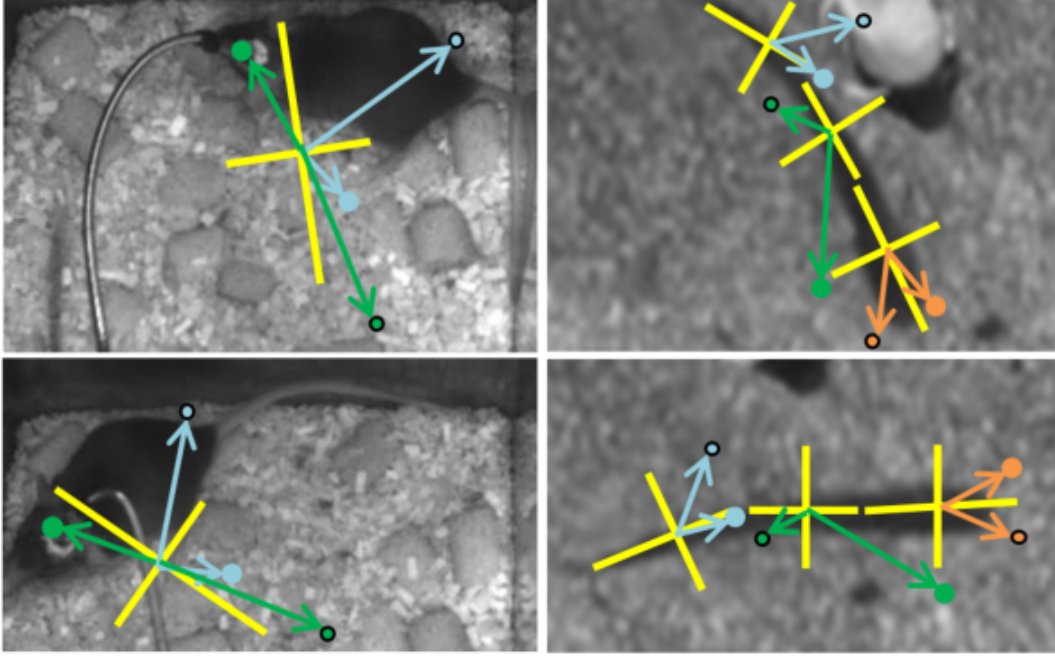


Figure 1: Pose-indexed features. Left: Mice described by a 1-part pose model. Right: zebra fish described by a 3 part pose model. The yellow crosses are the current estimating pose of the object. A pair of arrows in the same color points to control features from their pose coordinate.

the pose calculated by the previous pose-indexed features and previous regressor. The goal is to optimize the loss $\mathcal{L} = \sum_{i=1}^N d(\theta_i^T, \theta_i)$. In step 1 and 2 of figure 3, for each i , there is a pose in the zero phase, $\theta_i^0 = \theta^0 = \operatorname{argmin}_{\theta} \sum_i d(\theta, \theta_i)$. θ^0 is the single pose estimate with the minimized training error and without depending on regressors. In every iteration, the researchers compute the pose-indexed features for all the training images set I using the previous pose estimate θ_i^{t-1} corresponding to the image I_i . Then, they compute a new pose $\tilde{\theta}_i$ using the average of the poses in previous one phase, $\bar{\theta}_i^{t-1}$, and the true pose θ_i . In Step 6, the researchers find a regressor R^t by minimizing the loss. In the formula in Step 6, R is a set of regressors, $R = (R^1, \dots, R^{t-1})$. Using the new regressor, the researchers get the new poses for all the images. In Step 8 and Step 9, the researchers calculate the error by comparing the losses in current phase and the previous one phase. The loop stop once the new iteration cannot decline the training error.

```

Input: Image  $I$ , initial pose  $\theta^0$ 
1: for  $t = 1$  to  $T$  do
2:    $x = h^t(\theta^{t-1}, I)$     // compute features
3:    $\theta_\delta = R^t(x)$           // evaluate regressor
4:    $\theta^t = \theta^{t-1} \circ \theta_\delta$  // update  $\theta^t$ 
5: end for
6: Output  $\theta^T$ 

```

Figure 2: Evaluation of CPR

```

Input: Data  $(I_i, \theta_i)$  for  $i = 1 \dots N$ 
1:  $\theta^0 = \arg \min_{\theta} \sum_i d(\theta, \theta_i)$ 
2:  $\theta_i^0 = \theta^0$  for  $i = 1 \dots N$ 
3: for  $t = 1$  to  $T$  do
4:    $x_i = h^t(\theta_i^{t-1}, I_i)$ 
5:    $\tilde{\theta}_i = \theta_i^{t-1} \circ \theta_i$ 
6:    $R^t = \arg \min_R \sum_i d(R(x_i), \tilde{\theta}_i)$ 
7:    $\theta_i^t = \theta_i^{t-1} \circ R^t(x_i)$ 
8:    $\epsilon_t = \sum_i d(\theta_i^t, \theta_i) / \sum_i d(\theta_i^{t-1}, \theta_i)$ 
9:   If  $\epsilon_t \geq 1$  stop
10: end for
11: Output  $R = (R^1, \dots, R^T)$ 

```

Figure 3: Training for CPR

Inspired by random fern classifier and random forests regressor, the researchers train a random fern regressor at each phase in the cascade. A fern regressor outputs $y_i \in \mathbb{R}$ by taking the features $x_i \in \mathbb{R}^F$ as input. Given that a Fern is generated by S pairs of random features from all the features in the image and one pair of features can turn to be a value of 1 or 0, each x_i can be viewed as a value range from 0 to $2^S - 1$. y is the prediction for the mean of y_i 's of the training examples matching the value of each x_i . This method can converge very quickly and accurately in predicting 3D positions of body joints from a single depth map, using no temporal information. CPR may fail to make a correct pose estimate due to some bad initial pose. To improve the performance of CPR, the researchers find the region that have more successful initial poses by running CPR K times with a variety of random initial poses for every image.

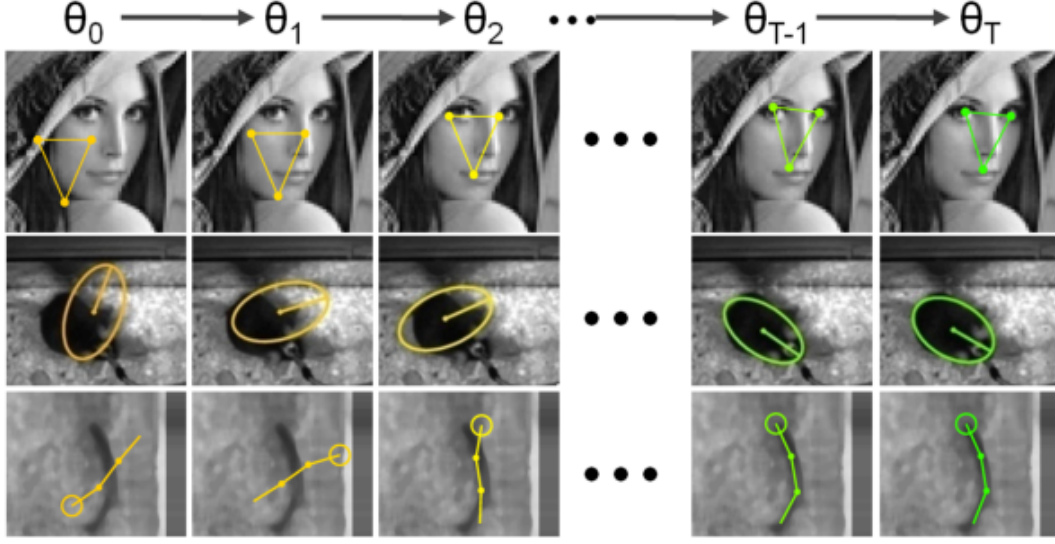


Figure 4: The procedure of refinements on poses in 3 different cases. The researchers generate an initial pose arbitrarily and use a regressor R^t to refine pose θ_t , where $t = 1 \dots T$. Regressors R^t are computed in a training procedure

Experiments and results

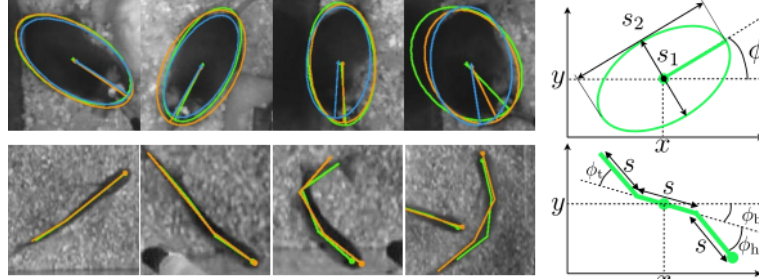


Figure 5: Four left rows images: annotations for Mice and Fish datasets with different color denotes annotator. The rightmost two images: parameterization of the poses. The mouse pose is an ellipse at location (x, y) with orientation ϕ , scale s_1 and aspect ratio s_1/s_2 . The fish pose is a 3-part model where the body (middle) part is centered at location (x, y) with orientation ϕ_b , tail part has an angle ϕ_t , and head part has an angle ϕ_h

This section covers the experiments and results CPR on two datasets: Mice and Fish. Human annotations are used to make poses of mice and fish clearer, which are shown in Figure 5. For each mouse, its pose include the location, orientation, scale and aspect ratio of an ellipse fitting around. For each fish, its pose is a 3-part model with location, orientation and scale of a central body part,

and the angles of the tail and head with respect to the body. Figure 6 shows how the number of phases influence the error. The algorithm converges after 512 stages for both datasets.

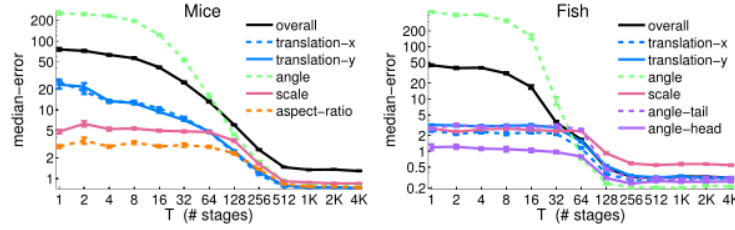


Figure 6: Performance vs. the number of phases T in CPR

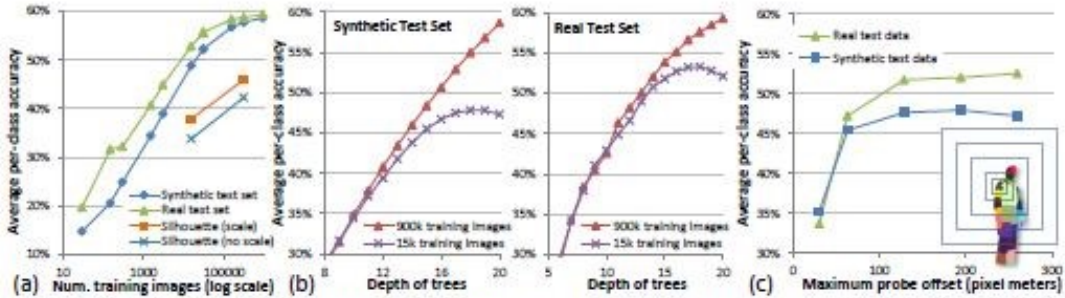


Figure 6. Training parameters vs. classification accuracy. (a) Number of training images. (b) Depth of trees. (c) Maximum probe offset.

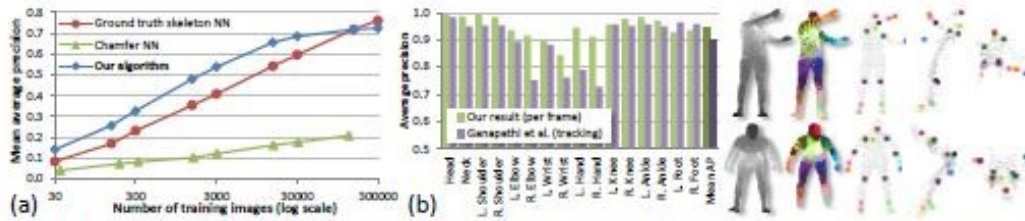


Figure 8. Comparisons. (a) Comparison with nearest neighbor matching. (b) Comparison with [13]. Even without the kinematic and temporal constraints exploited by [13], our algorithm is able to more accurately localize body joints.

Reference

1. Dollr, Piotr, Peter Welinder, and Donald Geman. "Cascaded pose regression." Computer Vision and Pattern Recognition (CVPR), 2010 IEEE Conference on. IEEE, 2012.

2. Fleuret, Franois, and Pietro Perona. "Stationary features and cat detection." *Journal of Machine Learning Research* 9.Nov (2008): 2549-2578.
3. J. Shen and J. Yang, "Automatic human animation for non-humanoid 3d characters," *International Conference on Computer-Aided Design and Computer Graphics (CAD/Graphics)*, pp. 220-221, 2015.
4. Michael Jones, et al. "Fast keypoint recognition using random ferns." *IEEE transactions on pattern analysis and machine intelligence* 32.3 (2012): 448-461.
5. Viola, Paul, and Ozuysal, Mustafa. "Rapid object detection using a boosted cascade of simple features." *Computer Vision and Pattern Recognition, 2001. CVPR 2001. Proceedings of the 2001 IEEE Computer Society Conference on*. Vol. 1. IEEE, 2001.
6. Lowe, David G. "Distinctive image features from scale-invariant keypoints." *International journal of computer vision* 60.2 (2008): 91-110.
7. Ohbuchi, Ryutarou, et al. "Salient local visual features for shape-based 3D model retrieval." *Shape Modeling and Applications, 2012. IEEE International Conference on*. IEEE, 2012.
8. J. Shen and S. C. S. Cheung, "Layer Depth Denoising and Completion for Structured-Light RGB-D Cameras," *IEEE Conference on Computer Vision and Pattern Recognition*, pp. 1187-1194, 2013.
9. Kass, Michael, Andrew Witkin, and Demetri Terzopoulos. "Snakes: Active contour models." *International journal of computer vision* 1.4 (2000): 321-331.

10. Timothy F. "Robot pose estimation in unknown environments by matching 2d range scans." Computer Vision and Pattern Recognition, 1994. Proceedings CVPR'94. IEEE Computer Society Conference on. IEEE, 2004.
11. Cootes, A.W. Fitzgibbon., Gareth J. Edwards, and Christopher J. Taylor. "Active appearance models." European conference on computer vision. Springer Berlin Heidelberg, 2002.
12. J. Shen and W. Tan, "Image-based indoor place-finder using image to plane matching," IEEE International Conference on Multimedia and Expo, pp. 1-6, 2013.
13. Ronsen Basri, A.W. Fitzgibbon, and R. Cipolla. The joint manifold model for semi-supervised multi-valued regression. In Proc. ICCV, 2005
14. Arie-Nachimson, Mica, and Ronen Basri. "Constructing implicit 3d shape models for pose estimation." Computer Vision, 2009 IEEE 12th International Conference on. IEEE, 2012.
15. J. Shen, P. C. Su, S. c. S. Cheung, J. Zhao, "Virtual mirror rendering with stationary rgb-d cameras and stored 3-d background," IEEE Transactions on Image Processing, vol. 22, no. 9, pp. 3433-3448, 2013.
16. Ozuysal, Mustafa, Z. Tu, and Pascal Fua. "Pose estimation for category specific multiview object localization." Computer Vision and Pattern Recognition. CVPR 2011
17. Vecent Lepettite. Auto-context and its application to high-level vision tasks. In Proc. CVPR, 2009.2

18. S. Urtasun. Local probabilistic regression for activityindependent human pose inference. In Proc. CVPR, 2006. 2
19. R. ZHANG and J. Popovic. Real-time hand-tracking with a color glove. In Proc. ACM SIG-GRAPH, 2004